THE JOURNAL OF BIOLOGICAL CHEMISTRY
Vol. 274, No. 32, Issue of August 6, pp. 22646–22651, 1999

Printed in U.S.A.

Nup192p Is a Conserved Nucleoporin with a Preferential Location at the Inner Site of the Nuclear Membrane*

(Received for publication, April 1, 1999, and in revised form, May 21, 1999)

Buket Kosova‡, Nelly Panté§, Christiane Rollenhagen§, and Ed Hurt‡¶

From the ‡Biochemie-Zentrum Heidelberg, Im Neuenheimer Feld 328, D-69120 Heidelberg, Germany and the §Institute of Biochemistry, Swiss Federal Institute of Technology (ETH), Universitätsstrasse 16, CH-8092 Zürich, Switzerland

Human Nup93, the homologue of yeast Nic96p, is associated with a 205-kDa protein whose intracellular location and function is unknown. We show here that the yeast open reading frame YJL039c, which is homologous to this human p205, encodes the so far largest yeast nucleoporin. Accordingly, green fluorescent protein (GFP)-tagged YJL039c was localized to the nuclear pores and therefore named Nup192p. Affinity purification of ProtA-Nic96p from glutaraldehyde-fixed spheroplasts reveals association with Nup192p. *NUP192* is essential for cell growth. A temperature-sensitive mutant nup192–15 is neither impaired in nuclear import of a SV40 nuclear localization sequence-containing reporter protein nor in mRNA export, but association of Nup49-GFP with nuclear pores is inhibited at the non-permissive temperature. By immunoelectron microscopy, Nup192p-ProtA is seen at the inner site of the nuclear pores, at a distance of 60 ± 15 nm from the central plane of the pore. This suggests that Nup192p is an evolutionarily conserved structural component of the nuclear pore complex with a preferential location at the inner site of the nuclear membrane.

The nuclear pore complexes are huge structures embedded in the nuclear membrane that provide the major route for the passive diffusion of small molecules and active transport of large molecules between the nucleus and cytoplasm (1–4). In the electron microscope, the nuclear pore complex displays a modular organization, consisting of an octasymmetrical framework of eight spokes sandwiched between cytoplasmic and nuclear rings (5). The spokes embrace a central channel or "transporter" which gates nucleocytoplasmic transport in both directions. Attached to this core structure are peripheral elements, the cytoplasmic pore filaments, which extend from the cytoplasmic ring, and the nuclear basket attached to the nuclear ring and consisting of eight filaments that end in a distal ring (6–9). Electron microscopy also showed that the 8-fold symmetry and modular aspects of pore complex organization have been conserved during evolution although yeast NPCs[1] are smaller as compared with *Xenopus* NPCs with respect to molecular mass and dimensions; in addition, some prominent structures present in vertebrates NPCs such as the luminal ring are absent in yeast (10, 11). The overall conservation in NPC morphology between yeast and vertebrates suggests that many components of the nuclear pore complex are conserved during evolution. Indeed, a significant number of NPC constituents are homologous between yeast and higher eukaryotes; however, often this homology is not easily noticed, and there are also cases in which no yeast homologue exists when a vertebrate Nup (*e.g.* Nup153) is known (12, 13). Conserved also is the machinery of soluble nucleocytoplasmic transport factors which interact with nucleoporins, in particular NPC constituents with FG/FXFG/GLFG repeat sequences (14). Accordingly, soluble transport factors such as importin/karyopherin α and β (Kap60p and Kap95p in yeast), the small GTPase Ran, and NTF2 have also been conserved in evolution (3).

One of the evolutionarily conserved subcomplexes of the nuclear pore is the Nsp1p complex in yeast and its higher eukaryotic counterpart, the p62 complex (12). In yeast, the core Nsp1p complex is built up by Nsp1p, Nup49p, and Nup57p (15), to which Nic96p is further attached (16). In vertebrates, the p62 complex consists of p62, p58, p54, and p45 (17), in which p62 and Nsp1p, p54 and Nup57p, and p58 and Nup49p show a distinct sequence similarity (12). Furthermore, yeast Nic96p has homologues in human and *Xenopus* which were named Nup93. Interestingly, human Nup93 was localized to the nuclear basket by immunoelectron microscopy, and immunoprecipitation with anti-Nup93 antibodies revealed interaction with a pool of p62 and a novel protein of 205 kDa (18). Recently, Nsp1p and its interacting partner Nic96p were located by immunoelectron microscopy to distinct sites within NPCs, *i.e.* at both sites of the central gated channel and at the terminal ring of the nuclear basket (11).

To further study the interaction of Nic96p with other nuclear pore proteins in yeast, we sought to analyze the putative *Saccharomyces cerevisiae* homologue (ORF YJL039c) of human p205, which is in a complex with Nup93 (18). We show here that YJL039c encodes the so far largest yeast NPC protein, which is essential for cell growth. By immunoelectron microscopy, Nup192p-ProtA was found to be localized at the nuclear basket. Temperature-sensitive mutants of nup192 reveal that the NPC reporter protein Nup49p-GFP was no longer assembled into nuclear pores. This suggests that Nup192p is a structural protein of the nuclear pores, most likely constituting a major component of the nuclear basket filaments.

EXPERIMENTAL PROCEDURES

Yeast Methods and DNA Recombinant Work—The yeast strains used in this study are listed in Table I. Cells were grown in minimal SDC or rich yeast extract/peptone/dextrose medium. Genetic manipulations of yeast were performed as described (19). The following yeast plasmids were used: pUN100, *ARS*/*CEN* plasmid with the *LEU2* marker; YCplac33, *ARS*/*CEN* plasmid with the *URA3* marker; YCplac22, *ARS*/*CEN* plasmid with the *TRP1* marker; pASZ11, *ARS*/*CEN* plasmid with the *ADE2* marker. Manipulation and analysis of DNA such as restriction analysis, end-filling, ligations, DNA sequencing, and polymerase chain reaction amplifications were performed according to Maniatis *et*

* The costs of publication of this article were defrayed in part by the payment of page charges. This article must therefore be hereby marked "*advertisement*" in accordance with 18 U.S.C. Section 1734 solely to indicate this fact.

¶ Recipient of a grant from the Deutsche Forschungsgemeinschaft (SFB352). To whom correspondence should be addressed. Tel.: 49 6221-54-41-73; Fax: 49 6221-54-43-69; E-mail: cg5@ix.urz.uni-heidelberg.de.

[1] The abbreviations used are: NPC, nuclear pore complex; ORF, open reading frame; GFP, green fluorescent protein; kb, kilobase(s); HA, hemagglutinin; ProtA, protein A; NLS, nuclear localization sequence.

TABLE I
Yeast strains

Strain	Genotype
RS453	*MATa/α, ade2/ade2, his3/his3, leu2/leu2, trp1/trp1, ura3/ura3*
BSY420	*MATa/α, ade2/ade2, his3/his3, leu2/leu2, trp1/trp1, ura3/ura3, can1/can1*
nup192$^-$/NUP192	*MATa/α, ade2/ade2, his3/his3, leu2/leu2, trp1/trp1, ura3/ura3, can1/can1, nup192::HIS3/NUP192* (BSY420 derived)
NUP192 shuffle	*MATa or α, ade2, his3, leu2, trp1, ura3, nup192:HIS3* (YCplac33-URA3-NUP192)
nup192–15	*MATa or α, ade2, his3, leu2, trp1, ura3, nup192:HIS3* (pUN100-LEU2-nup192–15 or YCplac22-TRP1-nup192–15)
NUP192-GFP	*MATa or α, ade2, his3, leu2, trp1, ura3, nup192:HIS3* (pUN100-LEU2-NUP192-GFP)
ProtA-NIC96	*MATa, ade2, his3, leu2, trp1, ura3, URA3-Pnop-ProtA-NIC96* (pUN100-LEU2-NUP192–HA)
nup133$^-$	*MATa or α, ade2, his3, leu2, trp1, ura3, nup133::HIS3*
nup192$^-$/nup133$^-$	*MATa or α, ade2, his3, leu2, trp1, ura3, nup192::HIS3, nup133::HIS3* (pUN100-LEU2-NUP192-GFP, pASZ11-ADE2)

al. (20). Gene disruptions were made by the one-step disruption method according to Rothstein (21).

Gene and Plasmid Constructions—The *NUP192* gene was excised from the cosmid clone cos82 (provided by Dr. Francis Galibert, Faculté de Médecine, Rennes, France) as a 7-kb *Stu*I/*Sph*I fragment and inserted into plasmid pUN100. To disrupt the *NUP192* gene, pUN100-NUP192 was cut with *Mlu*I/*Sna*BI, and a 5.65-kb fragment corresponding to the *NUP192* gene was released and replaced by the *HIS3* gene. It was cut with *Sph*I/*Eco*RI that released a 2.3-kb fragment, containing the *HIS3* gene and flanked by 0.5-kb 5′- and 0.6-kb 3′-untranslated region of *NUP192*. This *nup192::HIS3* fragment was used to transform the diploid BSY420 strain for homologues recombination. A haploid *nup192::HIS3* shuffle strain was constructed which was complemented by plasmid-borne YCplac33-URA3-NUP192. For tagging of Nup192p at its C-terminal end, a *Not*I site was created just before the stop codon of *NUP192* by a PCR-based method. Three tandem HA epitope tags or the ProtA tag, available as *Not*I restriction fragments (kindly provided by Dr. E. Schiebel, MPI, Munich, Germany), were inserted in-frame into the *Not*I site within *NUP192*. Accordingly, plasmids pUN100-NUP192-HA and pUN100-NUP192-ProtA were obtained. In a similar way, pUN100-NUP192-GFP and pUN100-NUP192-TEV-ProtA constructs were made. All constructs could complement the *nup192::HIS3* disrupted strain and thus were functional. For hydroxylamine-induced mutagenesis of *NUP192*, 20 μg of pUN100-NUP192 was incubated in 0.5 ml of hydroxylamine solution (0.45 M NaOH, 1.73 M hydroxylamine, 1 mM EDTA, pH 8.0) for 1 day at 55 °C.

Affinity Purification of ProtA-Nic96p and Nup192p-ProtA—Affinity purification of ProtA-Nic96p from yeast spheroplasts cross-linked with 0.1% glutaraldehyde was done as follows: a yeast strain expressing ProtA-NIC96 (16) was transformed with plasmid pUN100-NUP192-HA. Spheroplasted cells were resuspended in sorbitol buffer and split into four 25-ml aliquots. Increasing concentrations of glutaraldehyde were added: 0, 0.01, 0.1, and 1%, and it was incubated for 30 min on ice. After two washing steps with sorbitol buffer, ProtA-Nic96p and Nup192p-ProtA affinity purification on IgG-Sepharose beads were done as described previously (22).The lysis buffer for spheroplasts expressing Nup192p-ProtA was 20 mM Tris-HCl, pH 8.0, 150 mM KCl, 5 mM $MgCl_2$ ± 1% Triton X-100.

Fluorescence Microscopy—To detect GFP *in vivo* in the fluorescence microscope, the GFP-signal was analyzed in the fluorescein channel of a Zeiss Axioskop fluorescence microscope. Pictures were taken with a Xillix Microimager CCD camera, and digital pictures were processed by the software program Openlab (Improvision, Coventry, UK).

Immunoelectron Microscopy—Immunoelectron microscopy of cells expressing Nup192p-ProtA was done according to Fahrenkrog *et al*. (11) with certain modifications. Namely, the Nup192p-ProtA spheroplasts were extracted with 0.07% Triton X-100 before labeling with the anti-protein A antibody directly conjugated with gold.

Miscellaneous—SDS-polyacrylamide gel electrophoresis, Western blotting, indirect immunofluorescence, and analysis of poly(A)$^+$ RNA export were performed as described earlier (23). Transmembrane prediction was done according to TMpred Software from EMBnet on the WWW.

RESULTS AND DISCUSSION

We recently reported that mammalian Nup93, the vertebrate homologue of yeast Nic96p, is associated with p205 (18). Because a *S. cerevisiae* ORF (YJL039c) is homologous to human p205 (18), we tested whether this yeast YJL039c encodes a homologue of human p205. Meanwhile, an uncharacterized *Schizosaccharomyces pombe* ORF (GenBank™ accession number 4176539) appeared in the data libraries which is significantly homologous to *S. cerevisiae* ORF YJL039c. This allowed multiple sequence alignment between the various yeast and higher eukaryotic p205-related ORFs (Fig. 1*A*). Interestingly, when the *S. cerevisiae* and *S. pombe* ORFs were analyzed for transmembrane segments, several potential membrane-spanning sequences were predicted (Fig. 1*B*). Accordingly, these proteins contain hydrophobic stretches of amino acids scattered along the entire protein sequence (see also later).

The yeast YJL039c gene encoding a 192-kDa protein (p192) was tagged with GFP. Fluorescence microscopy of p192-GFP revealed a punctate nuclear envelope location with a staining pattern highly resembling the *in vivo* labeling of *bona fide* GFP-tagged nucleoporins (Fig. 1*C*). To demonstrate that p192 physically associates with nuclear pores in yeast, p192-GFP was expressed in nup133$^-$ cells which have clustered nuclear pores (24). p192-GFP co-clusters with nuclear pores in nup133$^-$ cells (Fig. 1*C*). Accordingly, p192 was named Nup192p. To find out about the *in vivo* role of *NUP192*, gene disruption of ORF YJL039c was performed. This showed that *NUP192* is essential for yeast cell growth (Fig. 2*A*). The lethal phenotype of the *nup192::HIS3* disruption mutant could be complemented by plasmid-borne *NUP192* or *NUP192-ProtA*. Thus, *NUP192* belongs to a group of nucleoporins that perform a unique and non-redundant function. In yeast, nucleoporins lacking FG-type repeat sequences are often not essential for cell growth (*e.g. NUP188, NUP170, NUP157, NUP133, NUP120, NUP85, NUP84, POM152*) and thus perform an overlapping function (25). The fact that *NUP192* has not shown up so far in genetic screens for overlapping or redundant interactions at the nuclear pores (*e.g.* synthetic lethal screens) may be explained by the difficulty in obtaining by random mutagenesis a specific mutation within the essential *NUP192* that causes synergistic impairment in combination with another mutated nucleoporin without completely inactivating the *NUP192* function. Furthermore, because no apparent defect in nucleocytoplasmic transport could be found in nup192 thermosensitive mutants, it makes sense in retrospect that nup192 mutants were not among mutant collections that are impaired in nuclear protein import and mRNA export.

To study the *in vivo* role of *NUP192*, several thermosensitive mutants of *NUP192* were generated by random mutagenesis (Fig. 2*B*). One of these thermosensitive mutants (nup192–15), which grows well at the permissive temperature (23 °C) and arrests at 37 °C (Fig. 2*B*, *lane 6*), was analyzed in more detail. The growth arrest was seen in nup192–15 thermosensitive mutants after an 8–10-h shift to the non-permissive temperature; accordingly, nuclear protein import of a classical NLS-containing GFP-reporter protein and Pus1p-GFP, as well as nuclear mRNA export, was analyzed in the nup192–15 thermosensitive mutant after a shift for several hours to the re-

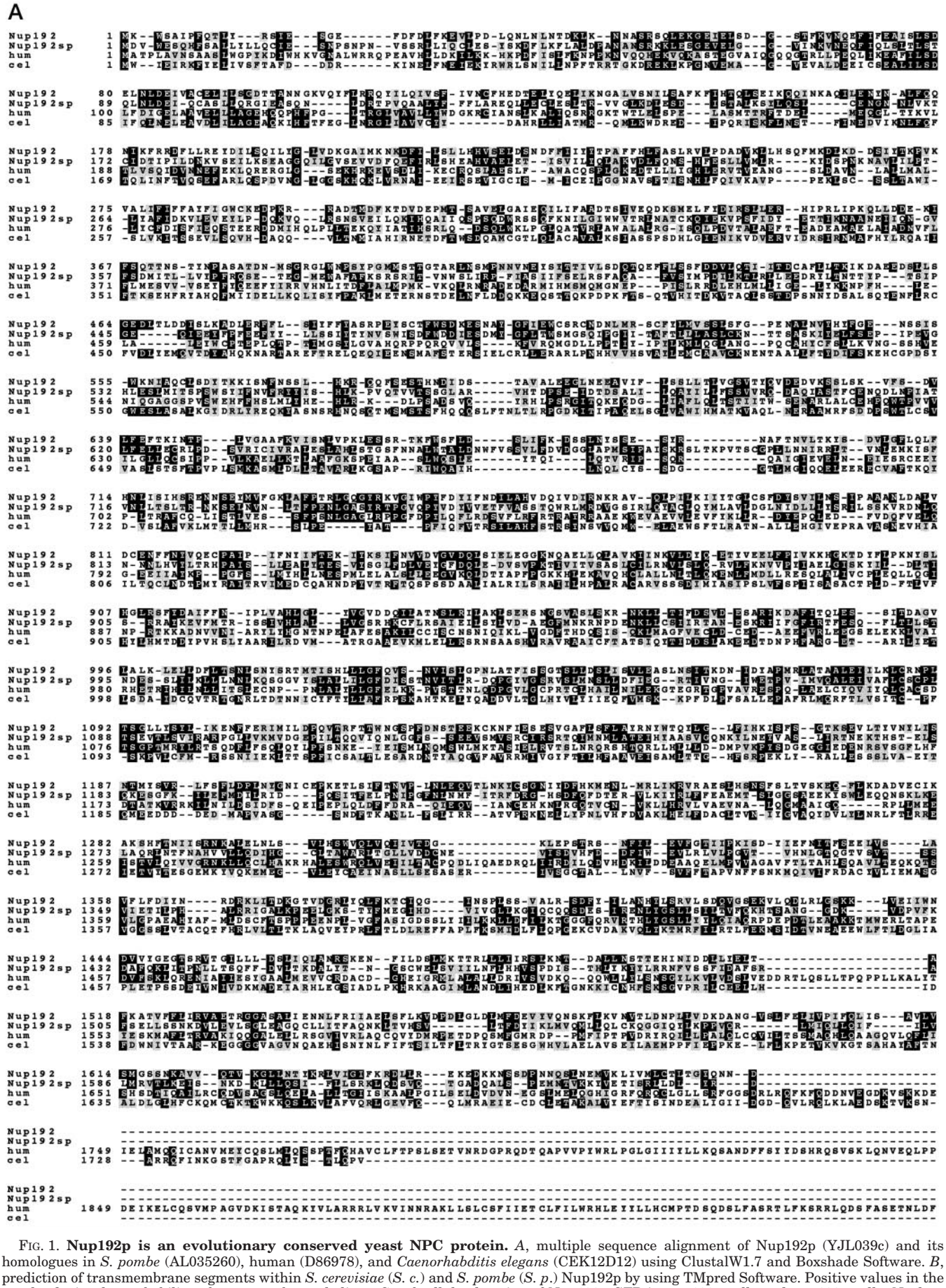

FIG. 1. **Nup192p is an evolutionary conserved yeast NPC protein.** *A*, multiple sequence alignment of Nup192p (YJL039c) and its homologues in *S. pombe* (AL035260), human (D86978), and *Caenorhabditis elegans* (CEK12D12) using ClustalW1.7 and Boxshade Software. *B*, prediction of transmembrane segments within *S. cerevisiae* (*S. c.*) and *S. pombe* (*S. p.*) Nup192p by using TMpred Software. Positive values in the graphs depict the probability of transmembrane helices. *C*, subcellular location of Nup192p-GFP in nup192^{-} cells and nup133^{-} cells. Nuclear envelope and nuclear pore location is revealed by fluorescence microscopy.

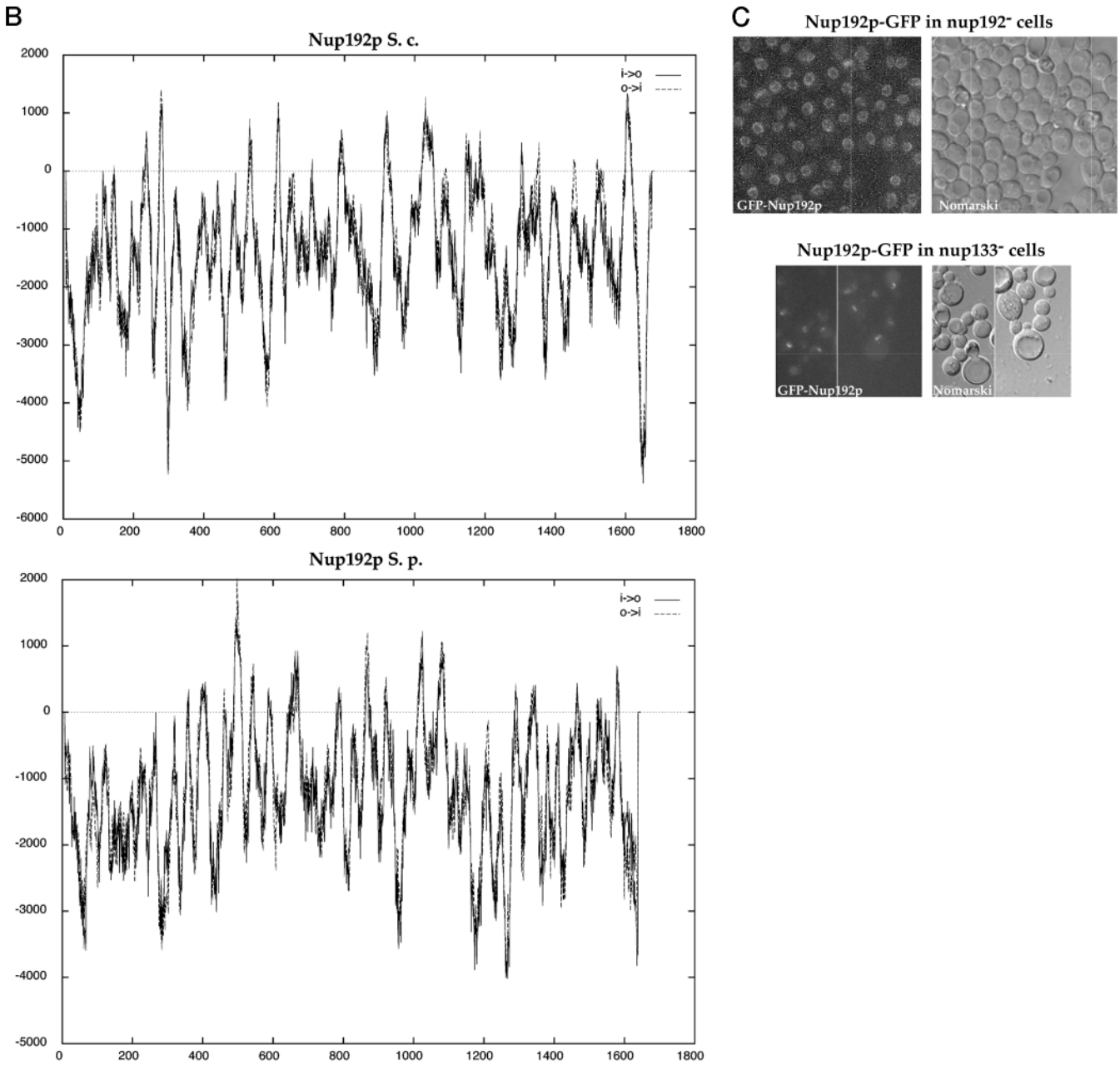

FIG. 1—*continued*

strictive temperature; however, no inhibition of these nuclear protein import pathways (Fig. 3A) and mRNA export (Fig. 3*B*) was noticed. It is worth mentioning that the nic96–1 thermosensitive mutant did not reveal defects in nuclear protein import and mRNA export, thus resembling the nup192–15 mutant (16, 26). Interestingly, the nic96–1 mutant is impaired in NPC biogenesis (26). We therefore tested whether the assembly of the NPC-associated protein GFP-Nup49p is altered in nup192–15 cells upon shift to the restrictive temperature. The punctate nuclear envelope signal of GFP-Nup49p significantly decreased after 8–10 h at 37 °C; in a few cells, aggregation of GFP-Nup49p was also noticed (Fig. 3*C*). As a control, nup192–15 cells complemented by plasmid-borne wild-type *NUP192* showed a normal nuclear envelope distribution and signal intensity of GFP-Nup49p when grown for 8–10 h at 37 °C (Fig. 3*C*). This suggests that assembly of GFP-Nup49p into the nuclear pores is impaired in the nup192–15 mutant. By using a similar fluorescence-based strategy, it was recently shown that certain NPC assembly mutants have a reduced GFP-Nup49p signal as compared with wild-type cells (27). We tested other GFP-tagged nucleoporins for the association with the nuclear envelope in nup192–15 *versus* NUP192$^+$ cells. In the case of Nic96p-GFP, Nup57p-GFP, and Nup82p-GFP, we also observed that the nuclear envelope location was significantly diminished at the restrictive temperature in nup192–15 as compared with NUP192$^+$ cells (data not shown).

To find out whether Nup192p is associated with Nic96p, ProtA-tagged Nup192p was affinity purified. Because the protein was predicted to contain eight strong transmembrane helices (see also Fig. 1*B*), we purified Nup192-ProtA in the absence and presence of 1% Triton X-100. However, under both conditions, Nup192p-ProtA could be purified similarly well, yielding Coomassie-stainable amounts (Fig. 4*A*, *lanes 9* and *10*). This suggests that Nup192p is not an integral membrane protein, and the presence of hydrophobic sequences may reflect a different structural feature than facilitating membrane insertion. Interestingly, Nic96p contains several hydrophobic stretches of amino acids in its primary sequence that are not

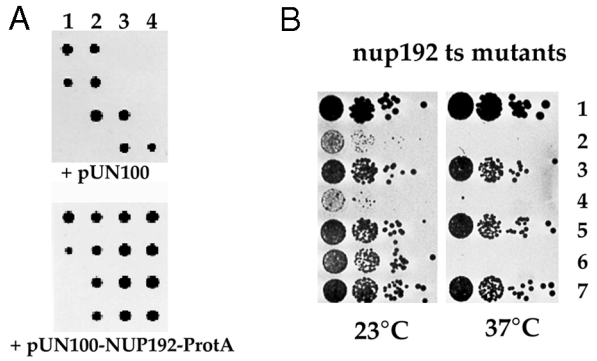

FIG. 2. **NUP192 is essential for yeast cell growth.** *A*, tetrad analysis of a heterozygous diploid strain disrupted for the ORF YJL039c (*nup192::HIS3*/*NUP192*$^+$). This revealed a 2:2 segregation for viability for the pUN100-transformed strain, but a 4:0 or 3:1 segregation, when plasmid-borne *NUP192-ProtA* was present (*lanes 1–4*, individual spores from complete tetrads). *B*, generation of temperature-sensitive nup192 mutants. The *NUP192* gene was mutagenized, and derived thermosensitive mutants (*nup192::HIS3* + pLEU2-nup192 ts) were characterized by growth on yeast extract/peptone/dextrose-plates at 23 °C (2 days) and 37 °C (3 days). *Lane 1*, wild-type (NUP192$^+$) strain; *lanes 2* and *3*, nup192–12 thermosensitive strain; *lanes 4* and *5*, nup192–13 thermosensitive strain; *lanes 6* and *7*, nup192–15 thermosensitive strain; *lanes 2, 4*, and *6*, cells lacking pURA3-NUP192; and *lanes 3, 5*, and *7,* cells carrying pURA3-NUP192. *ts*, thermosensitive.

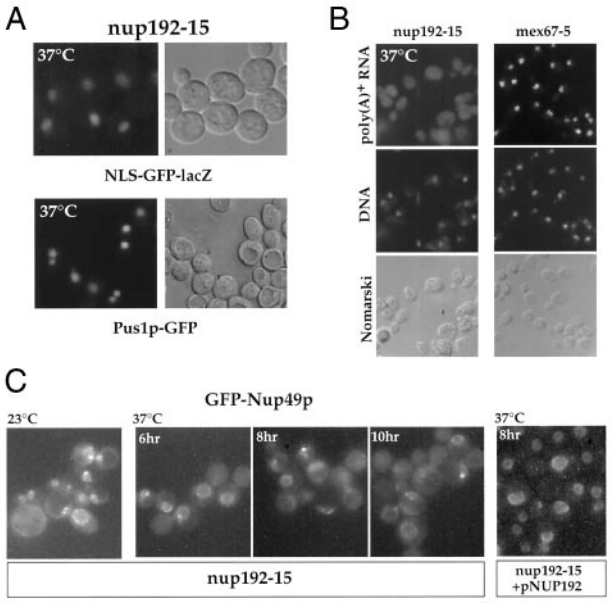

FIG. 3. **The thermosensitive nup192–15 mutant is impaired in assembly of GFP-Nup49p into nuclear pores.** *A*, analysis of nuclear protein import in nup192–15 cells. Nuclear accumulation of the nuclear reporter proteins SV40 NLS-GFP-lacZ and GFP-Pus1p in nup192–15 thermosensitive cells was measured after shifting the cells for 8 h to 37 °C. *B*, analysis of mRNA export in nup192–15 cells shifted for 3 h to 37 °C by *in situ* hybridization using a fluorescently labeled oligo(dT) probe. Cells were also stained for DNA, and Nomarski pictures were taken. As a control served the mex67–5 thermosensitive mutant which is strongly impaired in mRNA export at the non-permissive temperature. *C*, analysis of GFP-Nup49p assembly into nuclear pores in nup192–15 cells. It was grown at the indicated temperatures and for the indicated times before pictures were taken. The nup192–15 thermosensitive mutant was also transformed with the wild-type *NUP192* gene inserted into a single copy *ARS*/*CEN* plasmid (pNUP192).

membrane-spanning helices, but mutations therein strongly impair the Nic96p function (16).

Affinity purified Nup192p-ProtA does not reveal a major band which could correspond to Nic96p (Fig. 4*A*, *Coomassie*). On the other hand, Nup192p-ProtA had the tendency to degrade during purification yielding many ProtA-containing breakdown bands, as revealed by Western blotting (Fig. 4*A*, *anti-ProtA*). This made it difficult to estimate by Western blotting whether Nic96p is present in the eluate in substoichiometric amounts. Therefore, we affinity purified ProtA-Nic96p and looked for co-purification of a HA-tagged version of Nup192p by Western blotting using anti-HA antibodies. In this case, a small pool of Nup192p-HA could be detected in the ProtA-Nic96 eluate (Fig. 4*B*). We fixed yeast spheroplasts with glutaraldehyde to stabilize protein complexes prior to affinity purification of ProtA-Nic96p. This allowed us to obtain a better co-enrichment of HA-tagged Nup192p in purified ProtA-Nic96p preparation derived from 0.1% glutaraldehyde-treated spheroplasts (Fig. 4*B*, *lane 7*). It appears that Nup192p was not chemically cross-linked to Nic96p because the putative cross-link product should migrate at ~300 kDa on the SDS-polyacrylamide gel. The band observed on the SDS-polyacrylamide gel migrates at ~190 kDa, which is the expected size of Nup192p-HA. Accord-

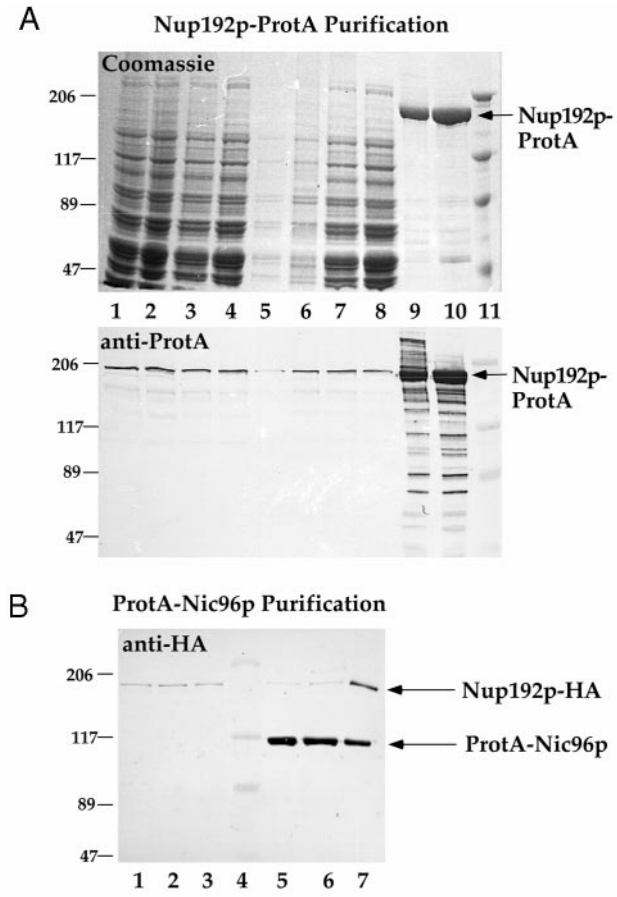

FIG. 4. **Purification of ProtA-Nic96p reveals interaction with Nup192p-HA.** *A*, affinity purification of Nup192p-ProtA by IgG-Sepharose chromatography was performed as described under "Experimental Procedures." The preparation was done in the absence (*lanes 2*, *4*, *6*, *8*, and *10*) and presence of 1% Triton X-100 (*lanes 1*, *3*, *5*, *7*, and *9*). A cell homogenate (*lanes 1* and *2*), soluble supernatant (*lanes 3* and *4*), insoluble pellet (*lanes 5* and *6*), flow through (*lanes 7* and *8*), and a 200-fold equivalent of (*lanes 9* and *10*) were analyzed by SDS-6% polyacrylamide gel electrophoresis, followed by Coomassie staining or Western blotting using anti-ProtA antibodies. A protein standard is also shown (*lane 11*). *B*, purification of ProtA-Nic96p from yeast spheroplasts which were incubated with different concentrations of glutaraldehyde. 25 μl of whole cell extracts (1–3) and derived affinity purified ProtA-Nic96p eluates (5–7) were analyzed by SDS-polyacrylamide gel electrophoresis followed by Western blotting using monoclonal anti-HA antibodies. *Lanes 1* and *5*, no glutaraldehyde; *lanes 2* and *6*, 0.01% glutaraldehyde; *lanes 3* and *7*, 0.1% glutaraldehyde; *lane 4*, high molecular weight protein standard (kDa). Note that anti-HA antibodies cross-react with the ProtA-moiety of ProtA-Nic96p.

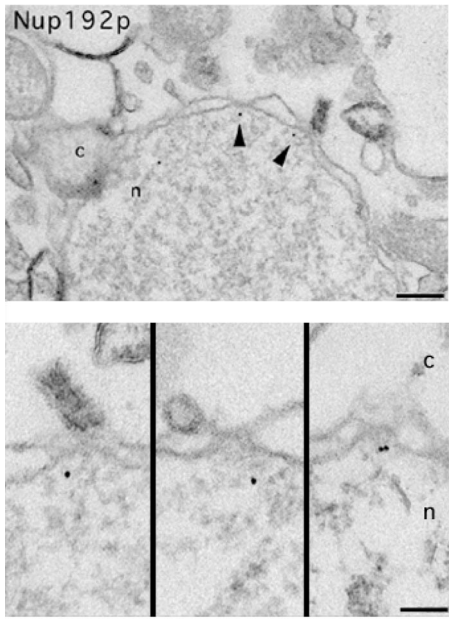

FIG. 5. **Immunoelectron microscopy localization of Nup192p-ProtA.** Nuclear cross-sections of ProtA-Nup192p pre-embedding labeled with anti-ProtA antibody directly conjugated to 8-nm colloidal gold particles (*top panel*) and gallery of selected examples of gold-labeled nuclear pore cross-sections from ProtA-Nup192p (*bottom panel*). Nup192p-ProtA was located at the nuclear periphery of the nuclear pore, at 60 ± 15 nm from the central plane of the pore. *c*, cytoplasm; *n*, nucleus. *Scale bar*, 200 nm (*top panel*) and 100 nm (*bottom panel*).

ingly, glutaraldehyde fixation can stabilize the physical interaction between Nic96p (or another member of the Nic96p complex) and Nup192p.

To determine the localization of Nup192p on the ultrastructural level, a strain expressing this protein tagged with ProtA was prepared by pre-embedding immunoelectron microscopy using a colloidal gold-conjugated anti-ProtA antibody (11). As seen in Fig. 5, the ProtA antibody labeled the nuclear periphery of the nuclear pores of ProtA-tagged Nup192p. For Nup192p, gold particles were detected at a distance of 60 ± 15 nm (mean ± S.D., $n = 19$) from the central plane of the pore. This suggests that Nup192p is an NPC protein with a preferential location at the nuclear basket. Accordingly, the pool of Nic96p, which is located at the nuclear basket by electron microscopy, may interact with Nup192p. An abundant labeling of ProtA-Nic96p at the nuclear basket and its terminal ring was previously found by immunoelectron microscopy (11). Similarly, human Nup93p is located at the nuclear basket (18) and physically associates with p205, the human homologue of Nup192p.

In conclusion, we have identified the so far largest yeast nucleoporin Nup192p which is likely to be the functional homologue of an evolutionarily conserved human protein (p205) that was found in association with human Nup93. This yeast Nup, although essential, escaped genetic screens so far. However, we could find it in an unusual way by employing reverse genetics that were based on the information available from p205, the potential human homologue of Nup192p. This assumption turned out to be correct and allowed us to identify a yeast nucleoporin on the basis of its sequence homology to its putative mammalian counterpart. All the subsequent work with yeast Nup192p revealed that it is a NPC protein and involved in the assembly of the NPC marker protein GFP-Nup49p into nuclear pores. The location of Nup192p at the nuclear basket and its interaction with the Nic96p complex finally led us to suggest that Nup192p and Nic96p are essential components of the nuclear basket and are required for NPC assembly. Finally, we propose that human Nup93 and its interacting protein, p205 (hNup192), perform a similar role in the higher eukaryotic cells.

Acknowledgements—We are grateful to members of the lab for critical reading of the manuscript.

REFERENCES

1. Cole, C. N., and Hammell, C. M. (1998) *Curr. Biol.* **8,** R368–R372
2. Mattaj, I. W., and Englmeier, L. (1998) *Annu. Rev. Biochem.* **67,** 265–306
3. Pemberton, L. F., Blobel, G., and Rosenblum, J. S. (1998) *Curr. Opin. Cell Biol.* **10,** 392–399
4. Stutz, F., and Rosbash, M. (1998) *Genes Dev.* **12,** 3303–3319
5. Panté, N., and Aebi, U. (1993) *J. Cell Biol.* **122,** 977–984
6. Goldberg, M. W., and Allen, T. D. (1992) *J. Cell Biol.* **119,** 1429–1440
7. Kiseleva, E., Goldberg, M. W., Daneholt, B., and Allen, T. D. (1996) *J. Mol. Biol.* **260,** 304–311
8. Panté, N., and Aebi, U. (1996) *Science* **273,** 1729–1732
9. Ris, H. (1997) *Scanning* **19,** 368–375
10. Yang, Q., Rout, M. P., and Akey, Ch. W. (1998) *Mol. Cell* **1,** 223–234
11. Fahrenkrog, B., Hurt, E. C., Aebi, U., and Panté, N. (1998) *J. Cell Biol.* **143,** 577–588
12. Doye, V., and Hurt, E. C. (1997) *Curr. Opin. Cell Biol.* **9,** 401–411
13. Shah, S., and Forbes, D. J. (1998) *Curr. Biol.* **8,** 1376–1386
14. Rexach, M., and Blobel, G. (1995) *Cell* **83,** 683–692
15. Grandi, P., Doye, V., and Hurt, E. C. (1993) *EMBO J.* **12,** 3061–3071
16. Grandi, P., Schlaich, N., Tekotte, H., and Hurt, E. C. (1995) *EMBO J.* **14,** 76–87
17. Guan, T., Müller, S., Klier, G., Panté, N., Blevitt, J. M., Haner, M., Paschal, B., Aebi, U., and Gerace, L. (1995) *Mol. Biol. Cell* **6,** 1591–1603
18. Grandi, P., Dang, T., Panté, N., Shevchenko, A., Mann, M., Forbes, D. J., and Hurt, E. C. (1997) *Mol. Biol. Cell* **8,** 2017–2038
19. Sherman, F. (1990) *Methods Enzymol.* **194,** 3–20
20. Maniatis, T., Fritsch, E. T., and Sambrook, J. (1982) *Molecular Cloning: A Laboratory Manual*, Cold Spring Harbor Laboratory Press, Cold Spring Harbor, NY
21. Rothstein, R. (1983) *Methods Enzymol.* **101,** 202–211
22. Santos-Rosa, H., Moreno, H., Simos, G., Segref, A., Fahrenkrog, B., Panté, N., and Hurt, E. (1998) *Mol. Cell. Biol.* **18,** 6826–6838
23. Segref, A., Sharma, K., Doye, V., Hellwig, A., Huber, J., Lührmann, R., and Hurt, E. C. (1997) *EMBO J.* **16,** 3256–3271
24. Doye, V., Wepf, R., and Hurt, E. C. (1994) *EMBO J.* **13,** 6062–6075
25. Fabre, E., and Hurt, E. (1997) *Annu. Rev. Genet.* **31,** 277–313
26. Zabel, U., Doye, V., Tekotte, H., Wepf, R., Grandi, P., and Hurt, E. C. (1996) *J. Cell Biol.* **133,** 1141–1152
27. Bucci, M., and Wente, S. R. (1998) *Mol. Biol. Cell* **9,** 2439–2461